Oral presentation | Industrial applications
Industrial applications-III
Tue. Jul 16, 2024 2:00 PM - 4:00 PM Room B

[5-B-03] Large-Eddy Simulation on Golf-Ball at supercritical Reynolds number and its comaprison with Smooth-Sphere

*Shota Nishinakagawa[1], Shushi Nakaoka[3], Masahide Onuki[2], Takahiro Sajima[2], Makoto Tsubokura[4] （1. Computational Fluid Dynamics Lab., Graduate School of System Informatics, Kobe University Graduate School., 2. Sumitomo Rubber Industries Ltd., 3. Computational Fluid Dynamics Lab., Computer Science and System Engineering, Kobe University Department., 4. Computational Fluid Dynamics Lab., Kobe University）

Keywords: Large-Eddy Simulation, Aerodynamics, Turbulence

Twelfth International Conference on Computational Fluid Dynamics (ICCFD12), Kobe, Japan, July 14-19, 2024

ICCFD12-2024-xxxx

Large-Eddy Simulation on Golf-Ball at supercritical Reynolds number and its comparison with Smooth-Sphere

Shota Nishinakagawa[*], Shushi Nakaoka[*]
Masahide Onuki[**], Takahiro Sajima[**]
and Makoto Tsubokura[*,***]
Corresponding author: nishinakagawa_s@stu.kobe-u.ac.jp

[*]Kobe University, Kobe, Hyogo, Japan
[**]Sumitomo Rubber Industries Ltd., Kobe, Hyogo, Japan
[***] RIKEN Center for Computational Science, Kobe, Hyogo, Japan

Abstract: In this work we present the results of an investigation of the aerodynamic characteristics of golf balls and smooth surface balls at supercritical Reynolds numbers using large eddy simulations (LES). The Reynolds number for the golf ball and the sphere where set to 110000 and 1140000, respectively. The aerodynamics characteristics of the two cases were found be significantly different leading to differences in lift and side force coefficients while drag force coefficients were found to be similar. The effect of spin on the flow characteristics of the two geometries are also investigated. We find different behaviour of the two geometries when subjected to rotation.

Keywords: Large-Eddy Simulation, Aerodynamics, Turbulence

1 Introduction

The characteristic feature of golf balls is the dimples embedded on their surfaces. Past studies have shown that the main role of these dimples is to reduce the critical Reynolds number from that of a smooth sphere [1]. Therefore, a question arises: do the same flow characteristics occur in a golf ball whose critical Reynolds number is artificially lowered, compared to a smooth ball that naturally reaches its critical Reynolds number? This work focuses on the differences in flow characteristics between a golf ball and a smooth sphere at the supercritical Reynolds number. A Large-Eddy Simulation using the dynamic Smagorinsky model was adopted to clarify the dominant flow characteristics around rotating and non-rotating balls.

2 Calculation Method

In the present study, a commercial golf ball, the Z-STAR (2013 model) made by Sumitomo Rubber Industries, and a smooth sphere with the same diameter as the golf ball are used. The governing equation solved in this study is the spatially filtered continuity and Navier-Stokes equations for incompressible flow, which were discretized using an unstructured mesh based on the finite volume method. The following is a filtered version of the continuity and the Navier-Stokes equations, where τ is called the Subgrid-scale stress.

$$\frac{\partial \overline{u_i}}{\partial x_i} = 0$$

$$\frac{\partial \overline{u_i}}{\partial t} + \frac{\partial \overline{u_i}\,\overline{u_j}}{\partial x_j} = -\frac{1}{\rho}\frac{\partial \bar{p}}{\partial x_i} + \nu\frac{\partial^2 \overline{u_i}}{\partial x_j^2} - \frac{\partial \tau_{ij}}{\partial x_j}\ , \quad \tau_{ij} = \overline{u_i u_j} - \overline{u_i}\,\overline{u_j}$$

To capture the change in flow from laminar to turbulent, a numerical mesh with 106 thin prism layers on the surface of the golf ball and 40 prism layers on the smooth spherical surface was used. The exterior of the prism layer consists of tetrahedral elements. The mesh resolution chosen for this work is based on the intensive grid resolution test carried out by Li et al. [2] to precisely capture the drag crisis of both smooth spheres and golf balls. The translation and rotation of the golf ball are

reproduced using the Arbitrary Lagrangian-Eulerian (ALE) method, wherein the entire numerical domain and the mesh move and rotate according to the geometry's motion. Consequently, an open-to-atmosphere boundary condition was applied to the outer boundary of the analysis region. The Reynolds number for the golf ball is set to 110,000, and for the smooth sphere, it is set to 1,140,000. The backspin when the ball is rotating is expressed by the dimensionless spin parameter Sp, given by $Sp = \pi DN/60U$ (where D is the golf ball diameter, U is the translational speed, and N is the rotational speed). For the simulations with rotating balls, Sp was set to 0.16.

3 Results

Drag coefficient C_D, lift coefficient C_L and side coefficient C_S are dimensionless force coefficients given by $C_D = F_D / 0.5\rho U^2 A$, $C_L = F_L / 0.5\rho U^2 A$ and $C_S = F_S / 0.5\rho U^2 A$ (F_D: drag force, F_L: lift force, F_S: side force, ρ: density, A: projected area).

	Golf ball Sp=0.00	Smooth sphere Sp=0.00
C_D	0.2144	0.2150
C_L	0.0571	-0.0969
C_S	0.0327	-0.1788

Table 1: Time averaged C_D, C_L and C_S of non-rotating balls

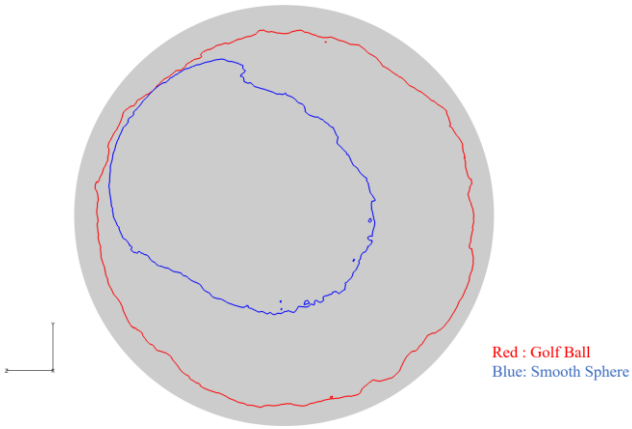

Figure 1: Time averaged separation line seen from behind the non-rotating balls

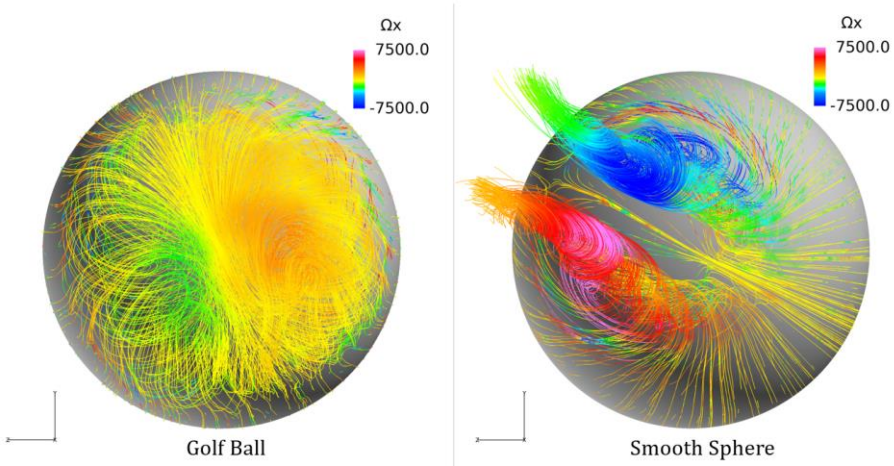

Figure 2: Time averaged streamline seen from behind the non-rotating balls
Ω_x indicates the vorticity of the longitudinal vortex, $\Omega_x = \frac{\partial v_z}{\partial v_y} - \frac{\partial v_y}{\partial v_z}$

Table 1 shows that the C_D values of a non-rotating golf ball and a non-rotating smooth sphere in the supercritical Reynolds are similar. However, C_L and C_s exhibit a very different behavior. Figure 1 shows the time averaged separation line. The separation line is a contour line where the translational velocity becomes zero. It can be seen that the separation line of the smooth sphere is much further back than that of the golf ball. It is generally known that drag decreases as separation retreats. Therefore, due to the relationship of the separation line, the C_D value of the smooth sphere should be smaller than that of a golf ball contrary to the obtained results. The reason for similar C_D values can be understood through Figure 2, where we can see that a strong vortex is generated behind the smooth sphere. This vortex causes induced resistance, and we found that the drag of the smooth sphere becomes as large as that of a golf ball. Furthermore, from Figure 2, we can see that the vortex that occurs on the smooth sphere is a stationary vortex. From Figures 1-3, we can see that the separation line of the smooth sphere is biased, resulting in greater lift and lateral force than a golf ball.

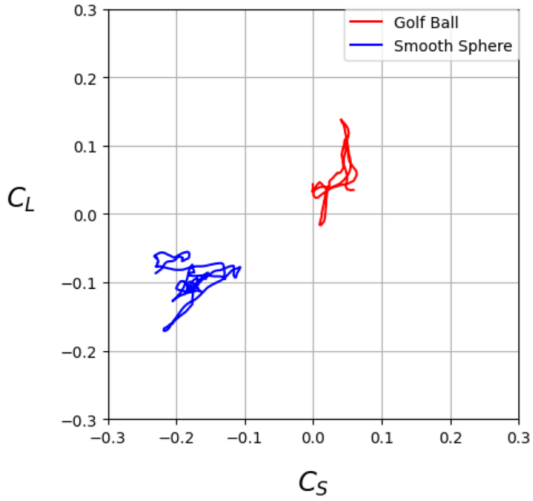

Figure 3: Time series C_S and C_L correlations of non-rotating balls.

Next, we compare the results when the balls are given a spin. The golf ball simulation was carried out for one rotation while the smooth sphere simulation was carried out for two rotations. Two rotations were necessary for the smooth sphere case to reach quasi steady state. Table 2 shows the time averaged C_D and C_L, and Figure 4 shows the time series of C_D and C_L of the two cases.

	Golf ball Sp=0.16	Smooth sphere Sp=0.16
C_D	0.2791	0.1491
C_L	0.2110	0.1097

Table 2: Time averaged C_D, and C_L of rotating balls

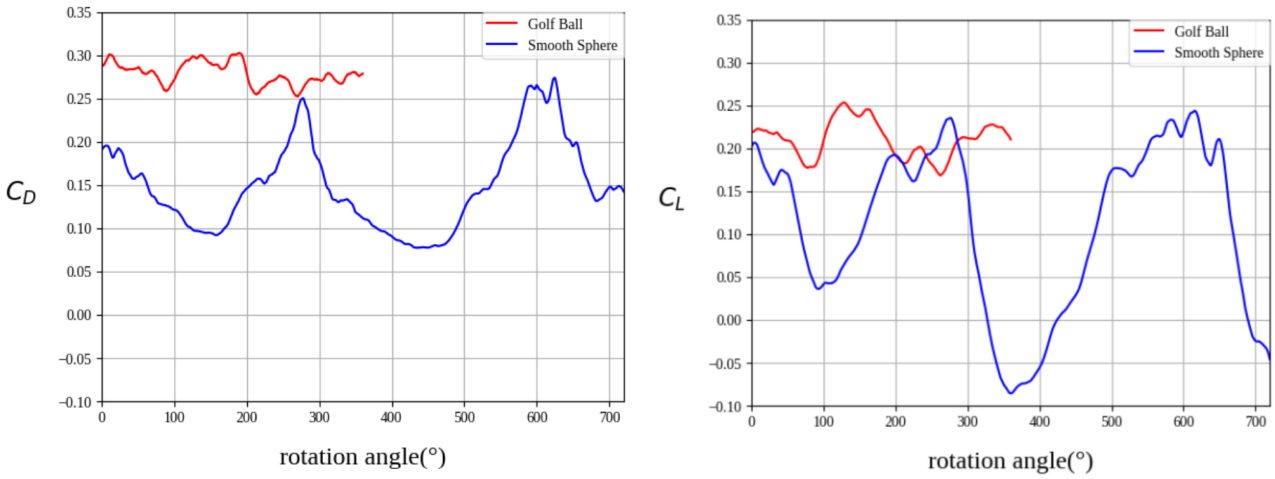

Figure 4: Time series of C_D and C_L of rotating balls

Table 2 shows that the C_D, which were about the same when there was no rotation, differs significantly when rotation is imposed. In addition to C_D, the lift coefficient (C_L) is also significantly different. This difference can be clearly seen in Figure 4, where the golf ball exhibits stable behavior, while the smooth sphere exhibits alternating Magnus effect and negative Magnus effect. The fact that both C_L values are larger than when there is no rotation is thought to be due to the Magnus effect. The reason why the C_L of a golf ball is larger than when there is no spin is due to the Magnus effect, while for the smooth sphere it is due to the sphere being subject to the Magnus effect while also being subject to the negative Magnus effect. Figure 5 shows the time-averaged streamlines of the golf ball and the smooth sphere. Comparing the golf ball in Figures 2 and 5, we can see that the rotation induces a strong coherent vortex behind the golf ball which leads to lower pressure on aft the golf ball resulting in an increase in C_D. On the other hand, the C_D of the smooth ball is smaller than that of the non-rotating ball because of the negative Magnus effect. From Figures 6 and 7, during the negative Magnus effect, the vortex weakens, the induced drag decreases, and the time-averaged C_D becomes smaller.

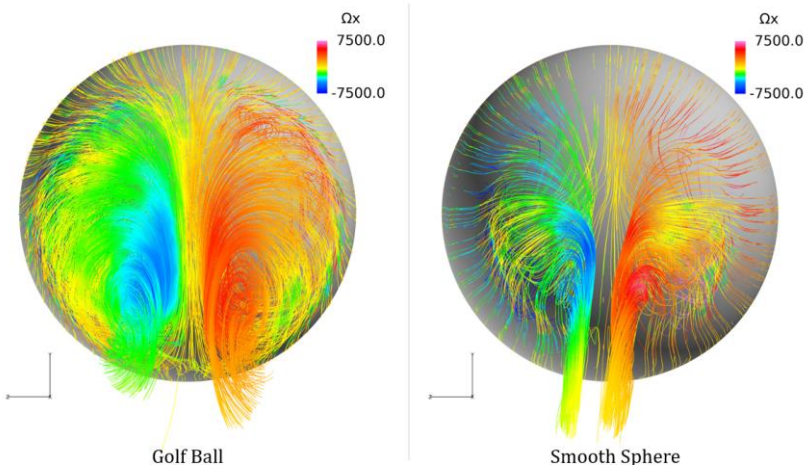

Figure 5: Time averaged streamline seen from behind the rotating balls
(Color bars are the same as in Figure 2)

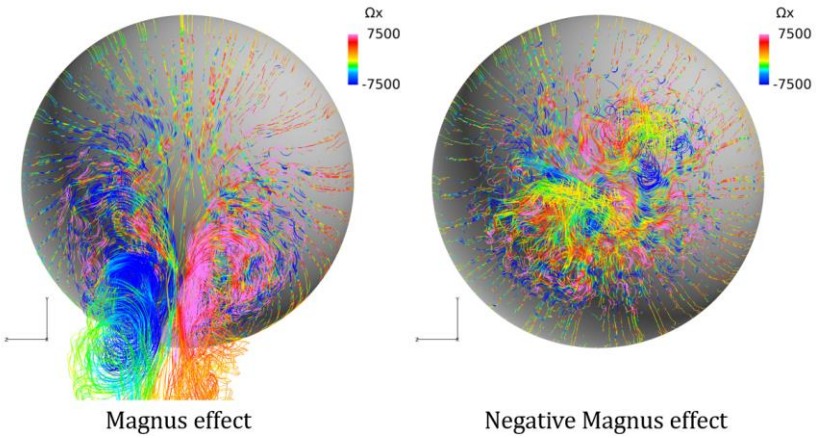

Figure 6: Streamlines seen from behind in the Magnus and negative Magnus effect on a rotating smooth sphere (Color bars are the same as in Figure 2)

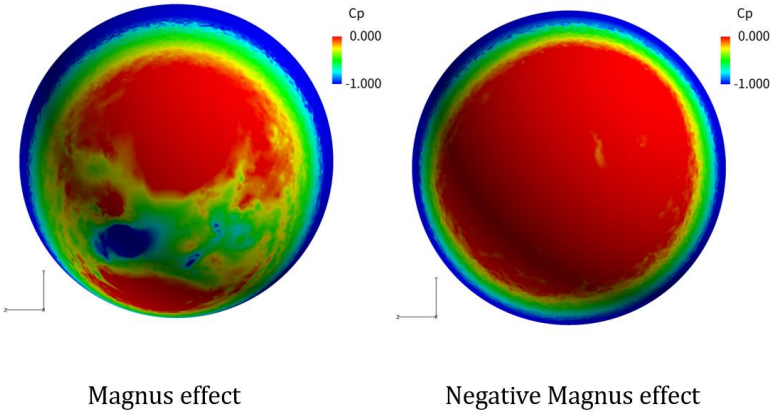

Figure 7: C_P values seen from behind during the Magnus effect and negative Magnus effect on a rotating smooth sphere ($C_P = (p - p_\infty) / 0.5\rho U^2 A$)

From Figure 8, it can be seen that in both cases, rotation causes the upper separation to retreat and the lower separation to advance slightly. Comparing it to Figure 1, it can be seen that in the case of the smooth sphere, the left/right bias is eliminated by rotation.

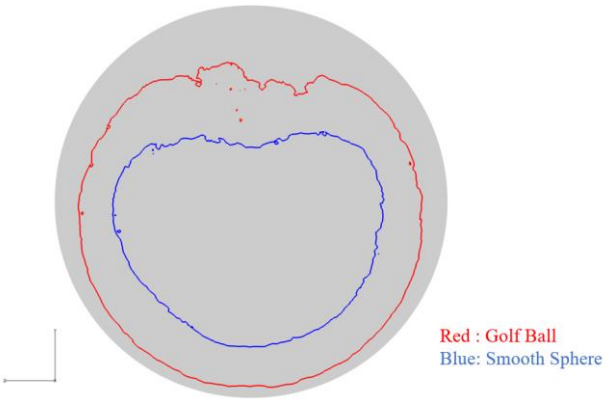

Figure 8: Time averaged separation line seen from behind the rotating balls

3 Summary

The aerodynamic characteristics of golf balls and smooth spheres investigated in this work were found to be significantly different for the two cases. While the drag coefficients of the two cases were similar, the lift and side force coefficients where significantly different due to differing wake patterns. When rotation is induced to the geometries the Magnus effect results in an increase in the lift coefficients of both the cases. However, an interesting phenomenon of negative Magnus effect observed in the smooth sphere case appears to significantly lower the drag coefficient. In contrast, the Magnus effect results in an increase in the drag coefficient of the rotating golf ball. In summary, the underlying aerodynamic characteristics of the smooth sphere and a golf ball (with an artificially lowered critical Reynolds number) at a supercritical Reynolds number were found to be significantly different. Even in the rotation cases, aerodynamic characteristics continued to differ, albeit for different reasons.

References

[1] Choi, J., Jeon, W. P. and Choi, H. (2006), "Mechanism of drag reduction by dimples on a sphere," *Physics of Fluids*, vol. 18, 041702.

[2] Li, J., Tsubokura, M. and Tsunoda, M. (2015), "Numerical Investigation of the Flow Around a Golf Ball at Around the Critical Reynolds Number and its Comparison with a Smooth Sphere," *Flow, Turbulence and Combustion*, vol. 95, pp. 415-436.